Manifestation of *PT* Symmetry Breaking in Polarization Space with Terahertz Metasurfaces

Mark Lawrence,[1] Ningning Xu,[2] Xueqian Zhang,[1,3] Longqing Cong,[3] Jiaguang Han,[3,*] Weili Zhang,[2,3,†] and Shuang Zhang[1,‡]

[1]*School of Physics and Astronomy, University of Birmingham, Birmingham B15 2TT, United Kingdom*
[2]*School of Electrical and Computer Engineering, Oklahoma State University, Stillwater, Oklahoma 74078, USA*
[3]*Center for Terahertz Waves and College of Precision Instrument and Optoelectronics Engineering, Tianjin University, Tianjin 300072, China*

(Received 14 April 2014; published 28 August 2014)

By utilizing the vector nature of light as well as the inherent anisotropy of artificial meta-atoms, we investigate parity time symmetry breaking in polarization space using a metasurface with anisotropic absorption, whose building blocks consist of two orthogonally orientated meta-atoms with the same resonant frequency but different loss coefficients. By varying their coupling strength, we directly observe a phase transition in the eigenpolarization states of the system, across which the long axis of the eigenpolarization ellipses experience a sudden rotation of 45°. Despite the lack of rotational symmetry of the metasurface, precisely at the phase transition, known as the exceptional point, the eigenmodes coalesce into a single circularly polarized state. The *PT* symmetric metasurfaces are experimentally implemented at terahertz frequencies.

DOI: 10.1103/PhysRevLett.113.093901 PACS numbers: 42.25.Bs, 78.20.Ci, 78.67.Pt

Parity time (*PT*) symmetric Hamiltonians have led to many interesting developments in theoretical physics. Most notably, these Hamiltonians, defined by an invariance under the simultaneous transformations of parity and time reversal, challenge a fundamental axiom of quantum theory stating that any physical observable must be represented by a Hermitian operator. While not necessarily Hermitian, a *PT* symmetric system could still possess a real and complete eigenspectrum and therefore still satisfies the necessary physical constraints for measurable quantities. Perhaps more interestingly, *PT* symmetric systems depending on an external parameter can also exhibit spontaneous symmetry breaking whereby the eigenspectrum suddenly transitions from real to complex [1].

Despite difficulties in precisely engineering quantum mechanical potentials, recently, *PT* symmetry breaking has been experimentally demonstrated in optics where the spatial profile of both real and imaginary parts of the dielectric function can be controlled almost arbitrarily. Initial studies have investigated the propagation of light through a pair of coupled waveguides with balanced loss and gain [2]. It has also been shown that *PT* symmetry breaking can occur in passive systems [3], which possess a loss contrast but no gain, allowing for simpler fabrication and characterization of *PT* structures. This can be understood by the fact that the passive system can be mapped back to the ideal case by a simple gauge transformation. As well as being of fundamental significance, these systems also exhibit potentially technologically important properties such as anomalous transparency, power oscillations, and unidirectional transparency [2–6]. More recently, *PT* symmetry has been explored in the spatiotemporal domain where spatially localized resonant states are coupled [7–12].

Metamaterials, artificial media composed of periodic arrangements of subwavelength meta-atoms, have revolutionized the fields of electromagnetism and optics. The versatility afforded by the design of these meta-atoms has revealed remarkable properties unseen in the natural world, such as negative refractive index and giant chirality, as well as novel applications, such as invisibility cloaks and superlenses [13–21]. Furthermore, it has been shown that metamaterials can significantly improve conventional optical devices via miniaturization and tunability [22,23]. Benefitting from the flexibility in combining unique structural effects with different constituent materials, metamaterials also provide an ideal platform for investigating novel physics related to symmetry and topology, which have prompted a number of recent theoretical and experimental investigations on *PT* symmetric metamaterials [24–27]. In this Letter we propose and demonstrate *PT* symmetry breaking in polarization space for a terahertz metasurface.

The metasurface comprises a 2D array of metamolecules, with each metamolecule consisting of two coupled Lorentzian dipoles $\hat{p}_{x,y} = \tilde{p}_{x,y}(\omega)e^{i\omega t}$ orientated along perpendicular directions and positioned in a mirror symmetric configuration, as shown in Fig. 1(a). There are two key advantages of using this configuration. First, the orthogonal orientation of the two sets of antennas allows us to probe the radiation field from each set independently. Second, and more importantly, the orthogonality of the two radiation fields ensures that the coupling coefficient between the two sets of antennas is real. Both dipoles resonate at the same frequency ω_0 and couple strongly to the incident radiation field $\hat{E}_0 = (\tilde{E}_x, \tilde{E}_y)e^{i\omega t}$; therefore, by working close to resonance ($\delta = \omega - \omega_0 \ll \omega_0$) and assuming that the dipole decay rates obey ($\gamma_y < \gamma_x \ll \omega_0$), the dipole moments of the antennas in the coupled system are related to the incident electric fields through the polarizability matrix as

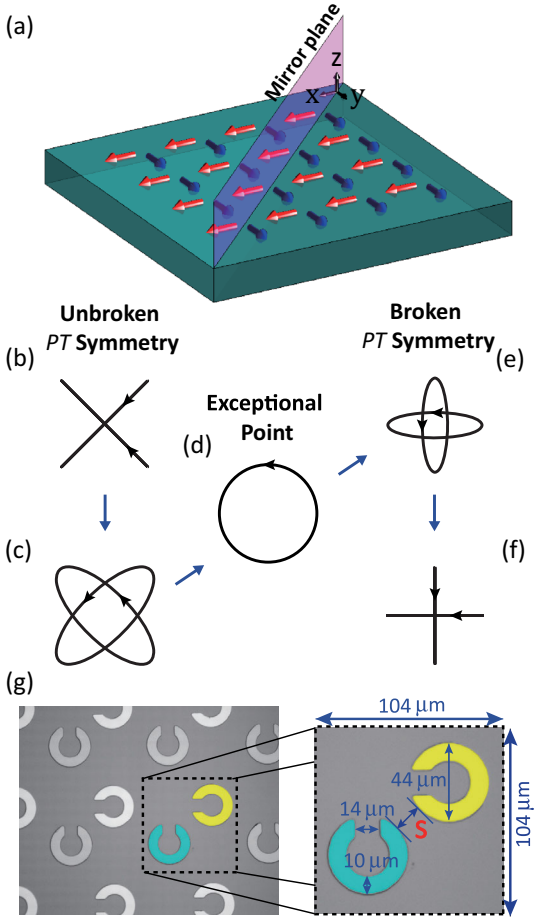

FIG. 1 (color online). *PT* symmetric dipole model and metasurface implementation. (a) Schematic of *PT* symmetric metasurface with less lossy dipoles (blue) and more lossy dipoles (red). (b)–(f) Eigenstates of Eq. (2) for varying G_{xy}, representing the eigenpolarization states of transmission through an ideal *PT* symmetric metasurface. (g) Photograph of *PT* symmetric metasurface composed of 300 nm thick silver (yellow or light gray) and lead (turquoise or dark gray) SRRs on silicon substrate.

$$\begin{pmatrix} \delta + i\gamma_x + G_{xx} & G_{xy} \\ G_{xy} & \delta + i\gamma_y + G_{yy} \end{pmatrix} \begin{pmatrix} \tilde{p}_x \\ \tilde{p}_y \end{pmatrix} = g \begin{pmatrix} \tilde{E}_x \\ \tilde{E}_y \end{pmatrix}, \quad (1)$$

where the coupling term G_{xy} is the summation of retarded fields from all of the $y(x)$ oriented antennas acting on an $x(y)$-oriented antenna, whereas $G_{xx} = G_{yy}$ is the summation of retarded coupling from all the other antennas oriented along the same direction. As mentioned previously, G_{xy} is real since the two sets of antennas radiate into orthogonal polarization states preventing radiative coupling. The transmitted field is simply the superposition of the incident field and the scattered field by the dipole antenna array in the forward direction [28], as

$$\begin{pmatrix} \tilde{E}_{tx} \\ \tilde{E}_{ty} \end{pmatrix} \equiv \overleftrightarrow{M} \begin{pmatrix} \tilde{E}_x \\ \tilde{E}_y \end{pmatrix} = \begin{pmatrix} \tilde{E}_x \\ \tilde{E}_y \end{pmatrix} + \frac{i\omega\eta_0}{2a^2} \begin{pmatrix} \tilde{p}_x \\ \tilde{p}_y \end{pmatrix}, \quad (2)$$

where $\eta_0 = \sqrt{\mu_0/\varepsilon_0}$ is the impedance of vacuum and a is the lattice constant of the metasurface. From Eqs. (1) and (2) it is obvious that the normalized eigenstates of the transmitted Jones matrix $\overleftrightarrow{M}$ are the same as those of the polarizability matrix. Thus, the eigenstates of the system can be analyzed simply using the polarizability matrix in Eq. (1). Similarly to previous works [3,6], our passive system, Eq. (1), can be separated into an anisotropic *PT* symmetric part and a lossy isotropic part:

$$S\overleftrightarrow{I} \begin{pmatrix} \tilde{p}_x \\ \tilde{p}_y \end{pmatrix} + \begin{pmatrix} -i\Gamma & G_{xy} \\ G_{xy} & i\Gamma \end{pmatrix} \begin{pmatrix} \tilde{p}_x \\ \tilde{p}_y \end{pmatrix} = g \begin{pmatrix} \tilde{E}_x \\ \tilde{E}_y \end{pmatrix}, \quad (3)$$

where $S = \delta + G_{xx} + i(\gamma_y + \gamma_x)/2$ and $\Gamma = (\gamma_y - \gamma_x)/2$. Although the physical system being considered here is a coupled set of lossy resonators, Eq. (3) could equally well describe an oscillator model with balanced loss and gain [second term on the left-hand side of Eq. (3)] embedded in a lossy background medium [first term on the left-hand side of Eq. (3)]. Note that the eigenstates of Eq. (3) are completely determined by the second term since the identity matrix in the first term does not affect the polarization eigenstates of the metasurface. It is obvious that the new polarization matrix, i.e., the matrix in the second term in Eq. (3), is *PT* symmetric, where *P* and *T* are represented by the Pauli matrix σ_x and complex conjugation, respectively.

Indeed, after direct diagonalization of the polarizability matrix in Eq. (1), variation of the coupling strength G_{xy} reveals a phase transition in the eigenstates of the system. Following Ref. [2], for $2G_{xy} > |\gamma_x - \gamma_y|$, known as the *PT* symmetric phase, resonant frequency splitting occurs and the eigenpolarization states of the metasurface are given by $(\hat{x} \pm e^{\pm i\theta}\hat{y})$, which are also eigenstates of the *PT* operator, where $\theta = \sin^{-1}[(\gamma_x - \gamma_y)/2G_{xy}]$. These polarization states correspond to two corotating ellipses with major axes oriented along $\pm 45°$, as shown in Figs. 1(b) and 1(c). For $2G_{xy} < |\gamma_x - \gamma_y|$, the resonance splitting is replaced by two modes at the same resonance frequency with differing rates of decay, and the eigenpolarization states are given by $(\hat{x} \mp ie^{\theta}\hat{y})$, which are exchanged under the operation of *PT*, where $\theta = \cosh^{-1}[(\gamma_x - \gamma_y)/2G_{xy}]$. These polarization states represent two corotating ellipses with major axes oriented along 0° and 90°, respectively, as shown in Figs. 1(e) and 1(f). By plotting the polarization eigenstates on the Poincaré sphere as a function of G_{xy} [Fig. (2)], it can be seen that *PT* symmetry breaking causes a sudden 45° rotation of the azimuthal angles despite the fact that the spatial symmetry of the polarizability matrix remains unaltered. The fact that both polarization eigenstates for a given set of parameters have the same rotation direction is a clear manifestation of the non-Hermitian nature of the system, as this means that, in general, the polarization eigenstates are nonorthogonal. At the exceptional point (EP) given by $2G_{xy} = |\gamma_x - \gamma_y|$, only a single left circularly polarized (LCP) solution exists, indicating that despite the lack of rotational symmetry, an LCP beam transmits through the

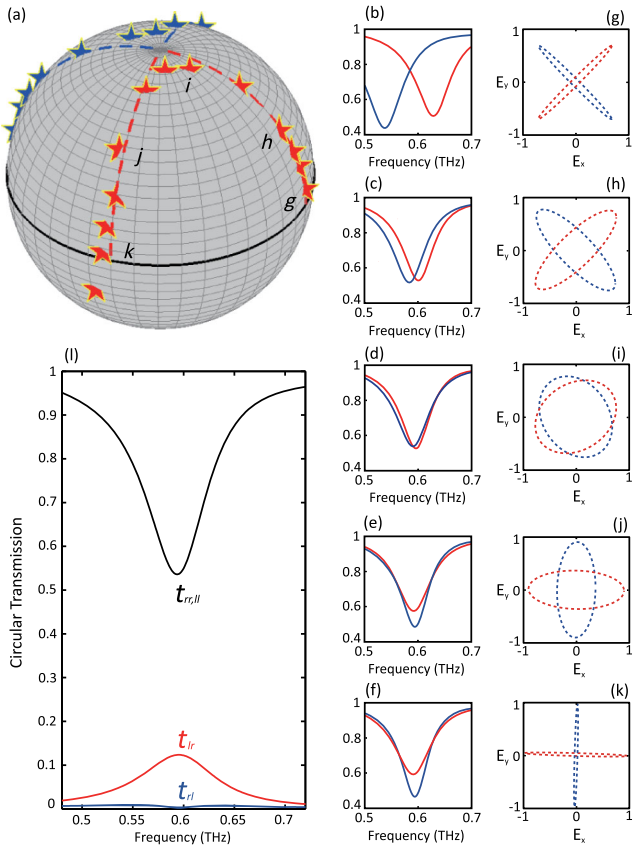

FIG. 2 (color online). Full-wave simulation results for a *PT* symmetric metasurface with variable coupling strength, controlled by changing the distance between more and less lossy SRRs between 2 and 20 μm. (a) Polarization eigenstates for different SRR separations plotted on the Poincaré sphere with LCP at the north pole, the dashed lines represent the eigenstates of an ideal *PT* symmetric dipole model with varying coupling coefficients and the single star occupying the southern hemisphere represents a change of sign of the coupling coefficient caused by the domination of the inductive coupling at large ring separation. Panels (b)–(f) show sampled transmission spectra for the eigenpolarization states (g)–(k) which correspond to points labeled in (a), ring separation in μm $= 2$ (b),(g), 12 (c),(h), 14.5 (d),(i), 16 (e),(j), 19 (f),(k). (l) Circular transmission spectra for SRR configuration closest to the EP (d),(i).

metasurface without any conversion to right circular polarization (RCP). Although the ellipticities of the polarization eigenmodes are themselves *PT* symmetric, the handedness of the EP can be changed by the action of a *P* or *T* transformation in isolation.

For implementation of the *PT* symmetry, we investigate a model system consisting of an array of orthogonally oriented split ring resonators (SRR). Each metamolecule consists of two geometrically identical SRRs 44 μm in diameter. The resonant frequency of a SRR is determined by its geometry in the terahertz regime, and so the use of two different metals, namely, lead and silver with different Ohmic loss, simply leads to a variation in linewidth for modes associated with the two rings. Benefitting from the capability of measuring both the phase and amplitude information of transmission for both polarizations using terahertz time domain spectroscopy, we are able to fully determine the polarization eigenstates of a *PT* metamaterial, which allows us to uniquely identify the interesting physics of *PT* symmetry breaking. Each SRR can be excited by an electric field across its gap; thus, it can be modeled as an electric dipole moment. When the two SRRs are placed in close proximity to each other, they interact through near-field coupling, which can be tuned by the separation between the two SRRs within each unit cell. Then by orientating the SRR split gaps along perpendicular directions, energy is radiated from the more lossy (lead) and less lossy (silver) SRRs into separate channels with orthogonal polarization states allowing the dynamics of the coupled system to be reflected in the complex transmission matrix. Clearly, this system obeys *PT* symmetry with respect to the plane ($y = -x$), and so by varying the ring separation, and therefore coupling strength, a phase transition should emerge.

We first study our metamaterial design numerically by carrying out full wave simulations using the commercial FDTD software CST MICROWAVE STUDIO™. The four complex transmission spectra, t_{xx}, t_{xy}, t_{yx} and t_{yy} are first calculated. Subsequently, the 2×2 transmission Jones matrix comprising the four complex coefficients can be diagonalized at each frequency. The eigenvalues of the transmission matrix and the corresponding polarization eigenstates are shown in Fig. 2 for SRR separations varying between 2 and 20 μm. As expected, a phase transition emerges, observable via both transmission spectra and polarization of the eigenstates. Below this transition the eigentransmission spectra, Figs. 2(b) and 2(c), reveal two resonant dips separated in frequency, which is a signature of the *PT* symmetric regime caused by splitting of the SRR dipole modes. On increasing the SRR separation, the spectral shift decreases until the EP is reached [Fig. 2(d)], where the two modes merge into one. Further increasing the SRR separation, *PT* symmetry breaking occurs, leading to identical resonance frequencies but a variation in linewidth for the eigenmode transmission spectra, as shown in Figs. 2(e) and 2(f).

As with the eigenvalues of a *PT* symmetric system, the corresponding eigenvectors also undergo a phase transition in terms of the amplitude and phase relationship between the two radiation channels. This relationship has direct consequences for the polarization response of our metamaterial structure. From Figs. 2(a), 2(g)–2(k), it can be seen that the shape of the polarization eigenstate ellipses in the broken and unbroken regimes possess distinct orientations of the major axis. In the strong coupling regime where *PT* symmetry persists, the polarization ellipses form with major axes orientated in $y = \pm x$; however, across the EP spontaneous *PT* symmetry breaking causes the eigenstates to rotate and align with the x and y axes. Interestingly, this phase transition in the electromagnetic response of our metamaterial results from simply changing the distance separating the two SRRs, and therefore no structural symmetries of the system are broken.

As previously mentioned, the EP separating these two distinct regions in parameter space is characterized by a coalescence of the eigenmodes. The coalescence is caused

by the singular nature of the coupling matrix and is an extreme consequence of the non-Hermiticity of the system. From Figs. 2(d) and 2(i) it can be seen that close to the EP the corotating polarization eigenstates of our metamaterial become almost circular. This behavior results in a highly asymmetric response to circularly polarized light with a very flat feature for t_{rl}, which has not previously been observed for normally incident illumination. Away from this region, the ellipticities, and therefore mode overlap, decrease on both sides of the transition and the two modes become orthogonal in both weak and strong coupling limits. Examination of Fig. 2(a) reveals a good correspondence between the simulation results and the simple dipole model except for a small anticrossing at the EP. Observations of both the chiral nature [29,30] of eigenvectors and anticrossing [31–35] close to an EP are consistent with previous microwave cavity experiments [30,31]. In Refs. [29–35] these phenomena are explained by the unique topology of a non-Hermitian parameter space, leading to the accumulation of a geometric phase by the eigenvectors upon circling once around an exceptional point. A *PT* symmetric transition is a special case of this in which the phases of the eigenvectors jump instantaneously by passing precisely through the singular parametric coordinate. In the present study, deviations from this sudden phase change can be attributed to a slight mismatch between the resonant frequencies of the individual SRRs, which is analyzed in more detail in the Supplemental Material [36].

In order to observe *PT* symmetry breaking experimentally, we have used photolithography to fabricate a number of metasurfaces with the separation between the silver and lead SRRs in each unit cell varying from 2 to 20 μm. Characterization was then performed using terahertz time domain spectroscopy giving both amplitude and phase information for both the co- and cross-linear polarization transmission coefficients (see Supplemental Material [36]). As with simulation, the spectral transmission data can then be diagonalized to reveal the eigenmodes of our metasurface (see Supplemental Material [36]), as presented in Fig. 3. After analyzing the measured results, a clear phase transition emerges whereby the spatial symmetry of the polarization eigenstates changes depending on whether or not *PT* symmetry is broken. For small ring separations the exact *PT* symmetric phase is occupied, as evidenced by spectral resonance splitting, which is accompanied by the predicted polarization response, symmetric about $y \approx \pm x$. On increasing the ring separation, spontaneous *PT* symmetry breaking causes spectral splitting to be replaced by relative broadening or narrowing of the two eigenmodes, as well as causing the orientation of the polarization eigenmodes to switch approximately to the x and y axes, corresponding to a 90° azimuthal rotation on the Poincaré sphere. By comparing Figs. 2(a) and 3(a) our measurements can be seen to agree well with simulation except for a more pronounced anticrossing at the EP, due to a mismatch in resonant frequencies associated with the silver and lead SRRs. This highlights the sensitivity of photonic systems close to an EP. The reason for this sensitivity stems from the diverging gradient of the eigenvalue caused by a square root

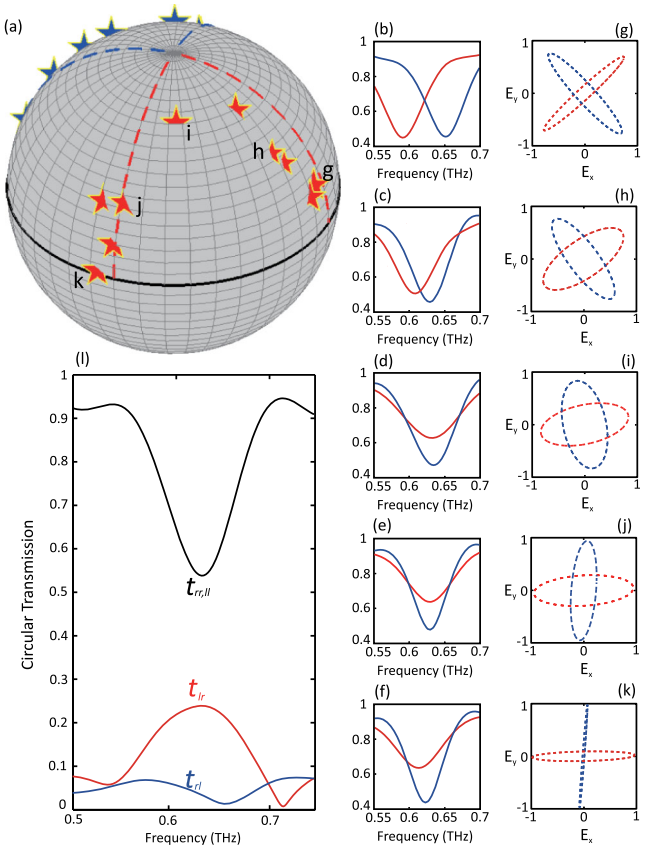

FIG. 3 (color online). Terahertz time domain spectroscopy measurements for a *PT* symmetric metasurface with variable coupling strength, controlled by changing the distance between lead and silver SRRs between 2 and 20 μm. (a) Polarization eigenstates for different SRR separations plotted on the Poincaré sphere with LCP at the north pole, the dashed lines represent the eigenstates of an ideal *PT* symmetric dipole model with varying coupling coefficients. Panels (b)–(f) show sampled transmission spectra for the eigenpolarization states (g)–(k) which correspond to points labeled in (a), nominal ring separation in μm = 2 (b),(g), 10 (c),(h), 11.5 (d),(i), 16 (e),(j), 20 (f),(k). (l) Circular transmission spectra for SRR configuration closest to the EP (d),(i).

dependence on the systems parameters. Nevertheless, the enhanced ellipticity of corotating states closest to the transition point still leads to strong asymmetric transmission for circularly polarized light.

Although the information presented in Fig. 3 is derived from the Cartesian transmission measurements rather than measured directly, the eigenstates of a system govern its polarization response to an arbitrarily polarized incident wave and are therefore crucial for understanding and controlling the transmission of light through anisotropic photonic media. This is evidenced by the strong asymmetric transmission of circularly polarized light in Fig. 3(l) close to the EP. Moreover, research into metasurfaces with spatially varying eigenpolarization states has recently revealed remarkable wave shaping functionalities including anomalous reflection and refraction [37], ultrathin tunable lenses [38], and holography [39], which may benefit from the discovery of polarization phase transitions.

In conclusion, we have investigated a novel phase transition in the polarization response of *PT* symmetric terahertz metasurfaces while crossing an EP. Spontaneous *PT* symmetry breaking, represented by a change in the orientation of the eigenpolarization ellipses, is observed both numerically and experimentally. Interestingly, the merging of the two eigenpolarization states into a single circular polarized state at the EP contradicts the conventional view that circularly polarized states only exist in structures with more than threefold rotational symmetries. While we have observed a *PT* symmetric phase transition in a coupled SRR array, it should be noted that this result is very general and should be realizable in any *PT* symmetric materials with anisotropic absorption. In fact, an effective medium approach would allow our metasurface to be described as a homogeneous layer with a permittivity tensor invariant under the same *P* and *T* operations as discussed here, and, therefore, our work has repercussions for the more general field of anisotropic photonic systems. Overall, our findings point to increased freedom for controlling the polarization of electromagnetic waves that goes beyond the apparent spatial symmetries.

We thank the financial support of EPSRC, NSFC (Grants No. 61328503, No. 11274207, No. 11104169, No. 61138001), National Basic Research Program of China (Grant No. 2014CB339800), NSF (Grant No. ECCS-1232081), and the Marie Curie Career Integration Program. We thank Lixiang Liu for her help with the graphics of the paper. M. L., N. X., and X. Z. contributed equally to this work.

*jiaghan@gmail.com
†weili.zhang@okstate.edu
‡s.zhang@bham.ac.uk

[1] C. M. Bender and S. Boettcher, Phys. Rev. Lett. **80**, 5243 (1998).
[2] C. E. Rüter, K. G. Makris, R. El-Ganainy, D. N. Christodoulides, M. Segev, and D. Kip, Nat. Phys. **6**, 192 (2010).
[3] A. Guo, G. J. Salamo, D. Duchesne, R. Morandotti, M. Volatier-Ravat, V. Aimez, G. A. Siviloglou, and D. N. Christodoulides, Phys. Rev. Lett. **103**, 093902 (2009).
[4] Z. Lin, H. Ramezani, T. Eichelkraut, T. Kottos, H. Cao, and D. N. Christodoulides, Phys. Rev. Lett. **106**, 213901 (2011).
[5] L. Feng, Y. L. Xu, W. S. Fegadolli, M.-H. Lu, J. E. B. Oliveira, V. R. Almeida, Y.-F. Chen, and A. Scherer, Nat. Mater. **12**, 108 (2013).
[6] A. Regensburger, C. Bersch, M.-A. Miri, G. Onishchukov, D. N. Christodoulides, and U. Peschel, Nature (London) **488**, 167 (2012).
[7] S. Bittner, B. Dietz, U. Günther, H. L. Harney, M. Miski-Oglu, A. Richter, and F. Schäfer, Phys. Rev. Lett. **108**, 024101 (2012).
[8] J. Schindler, A. Li, M. C. Zheng, F. M. Ellis, and T. Kottos, Phys. Rev. A **84**, 040101(R) (2011).
[9] Y. D. Chong, L. Ge, and A. D. Stone, Phys. Rev. Lett. **106**, 093902 (2011).
[10] S. Longhi, Phys. Rev. A **82**, 031801(R) (2010).
[11] M. Kang, F. Liu, and J. Li, Phys. Rev. A **87**, 053824 (2013).
[12] B. Peng, Ş. Kaya Özdemir, F. Lei, F. Monifi, M. Gianfreda, G. Lu Long, S. Fan, F. Nori, C. M. Bender, and L. Yang, Nat. Phys. **10**, 394 (2014).
[13] R. A. Shelby, D. R. Smith, and S. Schultz, Science **292**, 77 (2001).
[14] V. M. Shalaev, Nat. Photonics **1**, 41 (2007).
[15] J. Valentine, S. Zhang, T. Zentgraf, E. Ulin-Avila, D. A. Genov, G. Bartal, and X. Zhang, Nature (London) **455**, 376 (2008).
[16] V. A. Fedotov, P. L. Mladyonov, S. L. Prosvirnin, A. V. Rogacheva, Y. Chen, and N. I. Zheludev, Phys. Rev. Lett. **97**, 167401 (2006).
[17] S. Zhang, Y. S. Park, J. Li, X. Lu, W. Zhang, and X. Zhang, Phys. Rev. Lett. **102**, 023901 (2009).
[18] D. Schurig, J. J. Mock, B. J. Justice, S. A. Cummer, J. B. Pendry, A. F. Starr, and D. R. Smith, Science **314**, 977 (2006).
[19] J. B. Pendry Phys. Rev. Lett. **85**, 3966 (2000).
[20] N. Fang, H. Lee, C. Sun, and X. Zhang, Science **308**, 534 (2005).
[21] X. Zhang and Z. Liu, Nat. Mater. **7**, 435 (2008).
[22] H. T. Chen, W. J. Padilla, J. M. O. Zide, A. C. Gossard, A. J. Taylor, and R. D. Averitt, Nature (London) **444**, 597 (2006).
[23] N. Yu and F. Capasso, Nat. Mater. **13**, 139 (2014).
[24] N. Lazarides and G. P. Tsironis, Phys. Rev. Lett. **110**, 053901 (2013).
[25] G. P. Tsironis and N. Lazarides, arXiv:1304.0556.
[26] G. Castaldi, S. Savoia, V. Galdi, A. Alú, and N. Engheta, Phys. Rev. Lett. **110**, 173901 (2013).
[27] Y. Sun, W. Tan, H.q. Li, J.Li, and H. Chen, Phys. Rev. Lett. **112**, 143903 (2014).
[28] S. A. Tretyakov, A. J. Viitanen, S. I. Maslovski, and I. E. Saarela, IEEE Trans. Antennas Propag. **51**, 2073 (2003).
[29] W. D. Heiss and H. L. Harney, Eur. Phys. J. D **17**, 149 (2001).
[30] C. Dembowski, B. Dietz, H.-D. Gräf, H. L. Harney, A. Heine, W. D. Heiss, and A. Richter, Phys. Rev. Lett. **90**, 034101 (2003).
[31] C. Dembowski, H.-D. Gräf, H. L. Harney, A. Heine, W. D. Heiss, H. Rehfeld, and A. Richter, Phys. Rev. Lett. **86**, 787 (2001).
[32] W. D. Heiss, Phys. Rev. E **61**, 929 (2000).
[33] H. L. Harney and W. D. Heiss, Eur. Phys. J. D **29**, 429 (2004).
[34] C. Dembowski, B. Dietz, H.-D. Gräf, H. L. Harney, A. Heine, W. D. Heiss, and A. Richter, Phys. Rev. E **69**, 056216 (2004).
[35] U. Guenther, I. Rotter, and B. F. Samsonov, J. Phys. A **40**, 8815 (2007).
[36] See Supplemental Material at http://link.aps.org/supplemental/10.1103/PhysRevLett.113.093901 for (i) experimental details regarding terahertz measurements and data processing, (ii) effective parameter retrieval for simulated and measured transmission data.
[37] N. Yu, P. Genevet, M. A. Kats, F. Aieta, J. P. Tetienne, F. Capasso, and Z. Gaburro, Science **334**, 333 (2011).
[38] X. Chen, Nat. Commun. **3**, 1198 (2012).
[39] X. Ni, A. V. Kildishev, and V. M. Shalaev, Nat. Commun. **4**, 2807 (2013).